The CABRI fast neutron Hodoscope: calibration campaign results

Vincent Chevalier, Salvatore Mirotta, Nathalie Monchalin, Jerome Guillot

The CABRI fast neutron Hodoscope: calibration campaign results

***Abstract*— The CABRI experimental pulse reactor, funded by the French Nuclear Safety and Radioprotection Institute (IRSN) is owned and operated by CEA. This pool type research reactor located on the Cadarache nuclear research center in southern France, is devoted to fuel safety studies. The CABRI International Program (CIP), managed by IRSN in the framework of an OECD/NEA agreement, consists in studying the behavior of irradiated Light Water Reactor fuel under Reactivity Initiated Accidents (RIA). For the purpose of this program, a huge renovation of the facility has been conducted since 2003 to 2015 both for regulatory and experimental needs. The CABRI Water Loop was then installed to ensure prototypical Pressurized Water Reactor (PWR) conditions for testing irradiated fuel rods.**

The hodoscope station implemented in the CABRI reactor is a unique online fuel motion monitoring system, operated by IRSN and dedicated to the measurement of the fast neutrons emitted by the tested fuel rodlet during the power pulse. It is one of the most distinctive features of the CABRI facility. The system is able to determine the fuel motion, if any, with a time resolution of 1ms and a spatial resolution of 3mm during the transient test. The hodoscope equipment has been upgraded as well during the CABRI facility renovation. This paper presents the main outcomes achieved during the hodoscope calibration campaign in order to determine the new sensitivity coefficients of the detectors. This campaign was performed into two phases: fresh UO_2 fuel rod irradiation in CABRI reactor, and then gamma spectrometry measurement on this irradiated rod performed in hot cells facility. The comparison between hodoscope neutrons profile and gamma-scanning allows to determine the hodoscope detectors sensibility coefficients.

***Index Terms*— CABRI, Hodoscope, RIA, fast neutron detection system, Calibration Campaign**

V. CHEVALIER[1], S. MIROTTA, N. MONCHALIN, J. GUILLOT

I. NOMENCLATURE

RIA: Reactivity Initiated Accident
CIP: CABRI International Program
PWR: Pressurized Water Reactor
IRIS: Installation for Radiography Imaging and Spectrometry
MCNP: Monte Carlo Neutrons and Particles
LECA : Laboratoire d'Examens des Combustibles Actifs (Active Fuel Exams Laboratory),a CEA facility
FC : Fission Chamber
PR : Proton Recoil

II. INTRODUCTION

For enhancing safety of nuclear power plants (NPP), the Nuclear Safety and Radioprotection Institute (IRSN) carries out experimental programs in order to improve the understanding of the fuel behavior under various accident situations. One of them is the CABRI International Program, managed and funded by IRSN under an OECD/NEA agreement, launched to study Reactivity Initiated Accidents (RIA) in representative PWR conditions.

The CABRI research reactor, a pool type reactor, is designed to submit a test rod placed into the center of the core to a RIA transient. The old experimental sodium loop, crossing axially the entire core, has been replaced by a pressurized water loop during the refurbishing phase, to reproduce the thermal hydraulic conditions of a Pressurized Water Reactor (PWR), for testing a fuel rod and its cladding under prototypical conditions of RIA accidents in PWRs.

The power transients are generated by a unique reactivity injection system of CABRI [1]. A strong neutronic absorber gas, the ^{3}He, is previously introduced inside 96 tubes (so-called "transient rods", visible in Figure 1) located within the core, replacing the same number of fuel rods. These transients rods can be pressurized at up to 15 bar of helium. The transient power pulse is operated by a fast depressurization of this strong

[1] V. Chevalier, S. Mirotta, N. Monchalin, J. Guillot, authors, were with IRSN/PSN-RES/SEREX/L2EP, Cadarache, Saint Paul Lez Durance 13115 FRANCE (emails: vincent.chevalier@irsn.fr, salvatore.mirotta@irsn.fr, nathalie.monchalin@irsn.fr, jerôme.guillot@irsn.fr)

neutron absorber towards a 1000l discharge tank, through two discharge lines (low and high flow rates), each one being equipped with a fast-opening valve followed by a controlled valve. The helium 3 ejection can lead to a reactivity injection up to 4 $ in a very short time (< 80 ms).
The CIP program performed in the CABRI facility is directed by IRSN that also make use of its own followings experimental devices:

- The test device implemented in the in pile experimental cell and housing the fuel rod to be tested.
- The IRIS facility, a nondestructive examination bench which allows performing pre and post examinations of the test rodlet (X-ray imaging (radiography and tomography) ; quantitative gamma scanning measurements).
- The Hodoscope, an online fuel motion measurement system, which aims at analyzing the fuel motion deduced from the detection of fast neutrons emitted by the tested rod, in real time (with a time step of 1ms) during the power transient test.

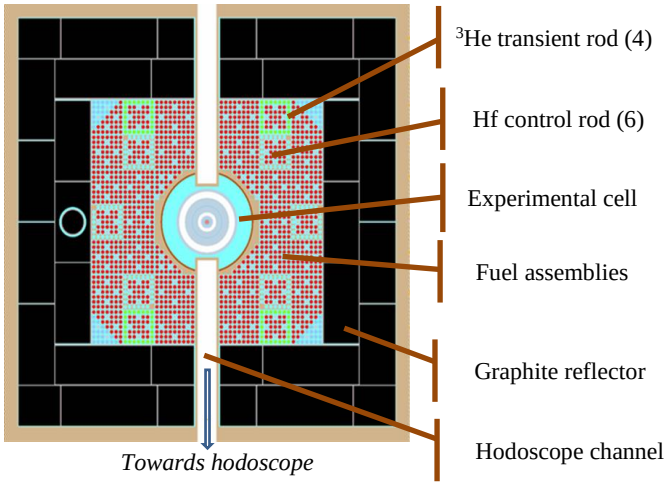

Figure 1: Cabri reactor Core

In section III of this article, a brief description of the hodoscope measuring system is given. In section IV, the methodology to determine the sensitivity coefficients of the hodoscope detectors is described. The axial power profiles of the calibration fuel rod, either deduced from neutrons measurements performed during steady power plateaus in CABRI reactor, or built from gamma detection realized in hot cell facility are respectively shown in section VI and in section VI. In section VII, the relation between hodoscope measurements and gamma spectrometry measurements is presented. The new sensitivity coefficients obtained as well as their uncertainties are presented in section VIII, in section 0. The validation of the results is demonstrated in section X. Finally a conclusion is given in section XI.

III. GENERAL DESCRIPTION OF THE HODOSCOPE SYSTEM

The hodoscope equipment is implemented in the CABRI facility since 1977. This system measures in real time the behavior of the test rod in the center of the CABRI core during a simulated accident. On CABRI reactor power plateau, the hodoscope is used to determine the fissile length and the axial power profile. During a power transient, the hodoscope is able to quantify the amount of fuel ejected in the milliseconds following failure, time-dependent axial fuel mass distributions and follow the fuel clusters after failure. In addition, the initial and final states of the test rod are precisely known thanks to the hodoscope measurements.
The hodoscope centerpiece is a massive stainless steel collimator of 3 m length (in green in Figure 2) made of 3 columns and 51 rows, so 153 measurement channels. Behind each one of these line-of-sights, a ^{237}Np fission chamber detector (FC) and a proton recoil proportional detector (PR) measure the fast neutrons coming from the core and test rod. Two different technologies of detectors are used in CABRI in order to follow all the experiments from low power (~50 KW) up to 20 GW. Proton recoil counters are better suited for low power (up to ~20 MW which means $3.5.10^{5}$ million impulsions per second without dead time

correction), thanks to its higher efficiency, whereas ^{237}Np fission chambers are used for higher power occurred during transient. The signal acquisition rate may be adjusted from 1 ms to 10 s according to the count rate.
The hodoscope collimator has three different degrees of freedom, for adjusting its position in front of the test rod. The distance between the collimator entrance face and the core axis may be adjusted manually in translation so as the geometrical efficiency is constant for all line of sights. Two direct current motors are used to move the collimator verticality and horizontally. Each one of the 306 detectors is linked by a µ-metal cable to its electronic chain placed 30 m far from the detector. These electronics have been renewed taking benefit of the renovation period [2].
In order to keep the noise due to neutrons coming from the driver core as low as possible, the reactor is crossed radially by the irradiation channel. In that way, none of the core fuel rods is in direct view to the hodoscope detectors. Nevertheless, the signal to noise ratio remains low (about 0.08 for proton recoil detectors and 0.20 for fission chambers) and requires specific data treatment algorithms.
The collimator was installed in order to “pixelize” the test rod placed in the center of the reactor. Each detector’s row looks at a slice of the test rod. In steady state conditions, the signals measured by all detectors are stable, whereas in transient conditions (i.e. a RIA pulse) they may vary according to a fuel displacement, a fuel densification (yielding to an increasing signal), or a fuel dilution or ejection (yielding to a decreasing signal).

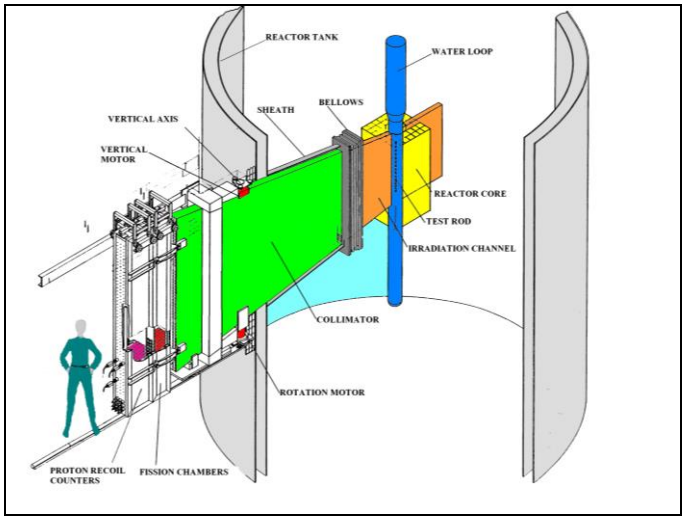

Figure 2 - Hodoscope detector system

IV. METHODOLOGY FOR CALIBRATION COEFFICIENT EVALUATION

During a fission event, several physical phenomena happen simultaneously:

- Production of radioactive fission products,
- Production of prompt neutrons,
- Production of prompt gamma,
- Production of neutrinos.

Subsequently, thanks to the radioactive decay, fission products emit several different particles like delayed neutrons, delayed mono-energetic gammas and other kind of particles. The calibration coefficient evaluation use both fast prompt neutrons emitted from the nuclear fission as well as the delayed gamma emitted from the fission products which are considered fuel tracers.
Fast neutrons are detected by the hodoscope measurement system. Detection efficiency depends on the intrinsic response of the detectors (placed in z) according to Equation 1.

$$T_m(z) = \varepsilon(z) \cdot T_r(z) \qquad \textbf{Equation 1}$$

- ε(z) is the efficiency of the detector,
- $T_r(z)$ is the real counting rate,
- $T_m(z)$ is the measured counting rate.

Furthermore the real counting rate which should be measured by the hodoscope fission chambers if the detection efficiency was equal to 1 is given by the fast neutrons coming from the test rod as shown in Equation 2.

$$T_r(z) = k.\nu \cdot \varphi_{th}(z) \cdot \sigma_{f,U35} \cdot N_{U235} \cdot V \qquad \textbf{Equation 2}$$

Where:

- $T_r(z)$: the real counting rate
- k: coefficient of proportionality taking into account the geometry of the system
- ν: the average number of neutrons emitted by fission
- $\varphi_{th}(z)$: the neutron thermal flux which creates fissions in the test rod
- $\sigma_{f,U235}$: is the microscopic cross section of fission for U^{235}
- N_{U235}: is the U^{235} concentration par unity of volume
- V: is the volumic section viewed by a row of the hodoscope

Moreover, considering ^{103}Ru as a fuel tracer produced only during reactor irradiation, the decrease in this isotope is negligible during reactor irradiation, we have:

$$\frac{dN_{Ru103}(z)}{dt} = \varphi_{th}(z) \cdot \sigma_{f,U235} \cdot N_{U235} \cdot \eta_{Ru103} \qquad \textbf{Equation 3}$$

Where η_{Ru103} is the fission yield of Ruthenium 103 per fission of Uranium 235.
So, if we consider the ^{103}Ru activity, we have:

$$A_{Ru103}(z) = \lambda_{Ru103} \cdot \varphi_{th}(z) \cdot \sigma_{f,U235} \cdot N_{U235} \cdot \eta_{Ru103} \cdot \Delta t \qquad \textbf{Equation 4}$$

Where·Δt is the irradiation time and λ_{Ru103} is the constant decay of the ^{103}Ru.
However, the ^{103}Ru has a $T_{1/2}$ period ($T_{1/2}$ = 1/λ) of 39.26 days (β-), that is to say much longer with respect to the irradiation time in the reactor (Δt << $1/\lambda_{Ru103}$). It is then possible to compare the activity of the ^{103}Ru measured at LECA, with the real counting rate of the detectors, $T_r(z)$ that is:

$$\frac{A_{Ru103}(z)}{\eta_{Ru103} \cdot \Delta t \cdot \lambda_{Ru103}} = \varphi_{th}(z) \cdot \sigma_{f,U235} \cdot N_{U235} = \frac{T_r(z)}{k.\nu.V} \qquad \textbf{Equation 5}$$

So:

$$A_{103_{Ru}}(z) = \alpha.T_r(z) \qquad \textbf{Equation 6}$$

So, the gamma activity measured in the hot cells facility (LECA of CEA) is proportional to the real counting rate of the detectors. The real counting rate is linked to the measured counting rate by Equation 1.
So, we have:

$$T_m(z) = \varepsilon(z) \cdot T_r(z) = \frac{\varepsilon(z)}{\alpha}.A_{103_{Ru}}(z) \qquad \textbf{Equation 7}$$

And:

$$S(z) = \frac{A_{103_{Ru}}(z)}{T_m(z)} \qquad \textbf{Equation 8}$$

Where S(z) is the proportional factor which is named “sensitivity factor”.

With an appropriate normalization it is possible to compare power profile measured by the hodoscope and radioactive profiles obtained by gamma spectrometry on Ru^{103} isotope.
Hence, the efficiency coefficient for the matrix detectors of the hodoscope system should be evaluated knowing the measured counting rate (this data can easily be obtained recording the counting rate with each detector when this one is placed in front of the test rod) as well as the activation profile of the test rod and compare them for each detectors.
Once irradiation campaign ended, the test rod was placed in front of a gamma spectrometer to count gamma emitted by fuel rod. By this way, it is possible to obtain an axial profile induced by irradiation in CABRI reactor.
The CH1 fuel test rod is made of fresh UO_2 (4.2% enrichment in U^{235}), with zircalloy 4 as cladding material and a fissile column length of 817mm.
The power profile, measured by gamma spectrometry, takes into account all the irradiation history of the test rod. For this reason, the irradiation profiles must be the same all over the test rod life. In Table 1, it is possible to see the irradiation history of the CH1 test rod. The average position of the 6 safety control rods (which may affect the axil power profiles) was $591.8\ \mathrm{mm}^{+8.1\ \mathrm{mm}}_{-3.6\ \mathrm{mm}}$ and the average power produced in the reactor was 10.2 MW ± 0.6 MW as well as the pressure of ^{3}He inside the transient rod was 10.000±0.005 bar.
The radiation profiles undergone by the calibration rod CH1 must be the same from one power plateau to another in order to faithfully reproduce the axial profile of the core.

Cycle length (s)	Core Power (MW)	Safety Control rods pos (mm/bfc)	Inlet Temp (°c)		Outlet temp (°c)		Flowrate (m3/h)	Date
			Start	End	Start	End		
1697	10.36	587.20	16.3	23.7	16.3	26.1	3180	26/06/17
2947	9.99	588.80	12.9	25.7	12.9	28.0	3180	27/06/17
2530	10.01	590.00	12.5	23.4	12.5	25.7	3150	28/06/17
6193	9.99	592.90	11.3	38.2	11.3	40.3	3175	29/06/17
5770	10.27	589.70	14.3	40.4	14.3	42.5	3200	6/07/17
2892	10.42	587.80	20.6	33.8	20.7	36.1	3190	3/10/17
792	9.74	593.50	34.2	38.4	34.3	38.9	3185	3/10/17
1101	10.49	585.30	13.3	17.9	13.3	19.5	3188	5/12/18
4508	10.12	589.50	19.1	38.5	19.1	40.6	3266	5/12/18
5469	10.17	600.90	15.9	39.9	16.0	41.9	3264	6/12/18
33899	10.16	591.7						6/12/18

Table 1: Irradiation history of CH1

V. ACQUISITIONS WITH THE HODOSCOPE DURING POWER PLATEAUS

The objective of the first phase of the acquisitions is to determine the positions "left", "center", "right", and "split" of the hodoscope collimator thanks to a power plateau at 10 MW. The “split” position corresponds to the position of the collimator between the “left” and “center” position.
To determine this position, the collimator must be rotated. Figure 2 shows the count rates measured by the left, center and right detectors of row 26 (row at mid-height of the hodoscope) during the rotation of the collimator. The three columns successively see the calibration rod, the core noise and the neutrons scattered by the pressurized water loop structural materials. Reading the maximum of each curve makes it possible to determine the position of the calibration rod when this latter is aligned with each column of detectors.

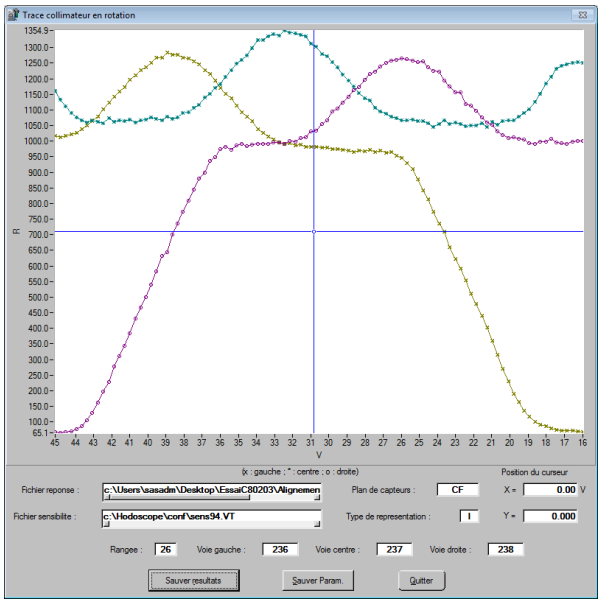

Figure 2: FC response from the row 26 during the collimator rotates

In Figure 3, the maximum count rate for each window of the hodoscope is presented according to the position of the collimator. This figure shows the positions of the rotation motor for which the calibration rod is seen by each column. The position of the rotation motor is expressed in Volts because this information is measured from a resistive position sensor. The analysis of these curves for each window of the hodoscope allows to determine the position of the collimator when this latter aims the calibration rod. So we are able to determine the “left”, “center”, “right”, and “split” (the average of “center” and “left” position) position of the collimator.

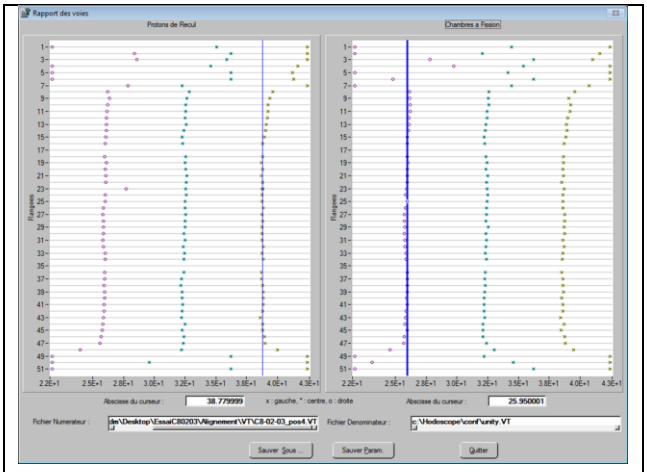

Figure 3: Visualization of the fissile column during the collimator rotation

Then, the position of the collimator is successively adjusted to the “left” position, to the “center” position, to the “right” position, and finally to the “split” position determined during the first step. For each position mentioned above, the duration of the acquisition at 10 MW is approximately 20 minutes.

VI. GAMMA SPECTROMETRY MEASUREMENTS

As told in section IV, after the irradiation in the CABRI reactor, the CH1 fuel rod was transported in the hot cells facility (LECA). After the unloading phase from the test device, the CH1 fuel rod was transferred on a Non Destructive Examination bench equipped with gamma spectrometry station. The gamma spectrometry measurements were performed and the decay has been taken into account. Fuel tracers were used to evaluate gamma profile shown in Figure 5. As explained in section IV, the aim is to compare the power profile measured by the hodoscope to the profiles obtained by gamma spectrometry on the chosen isotope. Indeed, it is necessary to compare each graph measured by the three columns of the hodoscope to a reference. This reference is given by the spectrometry measurement obtained in LECA facility.

All of these nuclei were measured (in keV):

La_140 (328.76)	LA_140 (487.02)	Ru_103 (497.0)	Ba_140 (537.2)	Ru_103 (610.33)	Ru_106 (621.9)
Cs_137 (661.66)	Zr_95 (724.19)	Zr_95 (756.7)	Nb_95 (765.8)	La_140 (815.78)	La_140 (1596.2)

The ^{137}Cs must be eliminated quickly. The exam cell is indeed too polluted by this element. The ^{137}Cs signal emitted by the CH1 rod is too low in comparison with the background noise of the cell.

^{106}Ru, ^{103}Ru (610keV), ^{140}Ba, rays and the 4 rays of ^{140}La were also not chosen because their counting rates were too low compared to the others counting rates available.
At that stage, the two ^{95}Zr rays, the ^{95} Nb ray could be used, as well as ^{103}Ru (497keV) ray. The ^{95}Zr rays were eliminated because of the possible zirconium activation phenomena. Zirconium is indeed contained in Zircalloy4 of the CH1 rod cladding.
The ^{95}Nb ray is also rejected, because it is a radioactive daughter of ^{95}Zr and so it ends to the same conclusion as for ^{95}Zr.
Finally, the 497 keV ray of ^{103}Ru will be used as reference for the calibration of the hodoscope.

The first treatment applied to LECA spectrometry results is the deletion of counts corresponding to the inter-pad spaces (i.e. sudden drop in the count rate). These count rates are then normalized with respect to the maximum count rates.
On the spectrometry graph (Figure 2), in the lower part of CH1 rod, for reactor dimension less than – 7222 mm[2], a breaking slope is observed, whose comes from a change in material nature at this point. Indeed, the materials of device surrounding the fuel rod is made of Zircalloy 4 alloy, whereas it is made of stainless steel in the lowest part. The irradiation of the fuel rod is therefore heterogeneous at this level. The gamma spectrometry values below this dimension are therefore not considered.
It is important to note that the measurements made at the LECA do not cover all the rows of the hodoscope, but only those between rows 9 to 47. The length of the calibration rod is indeed shorter than the collimator elevation.

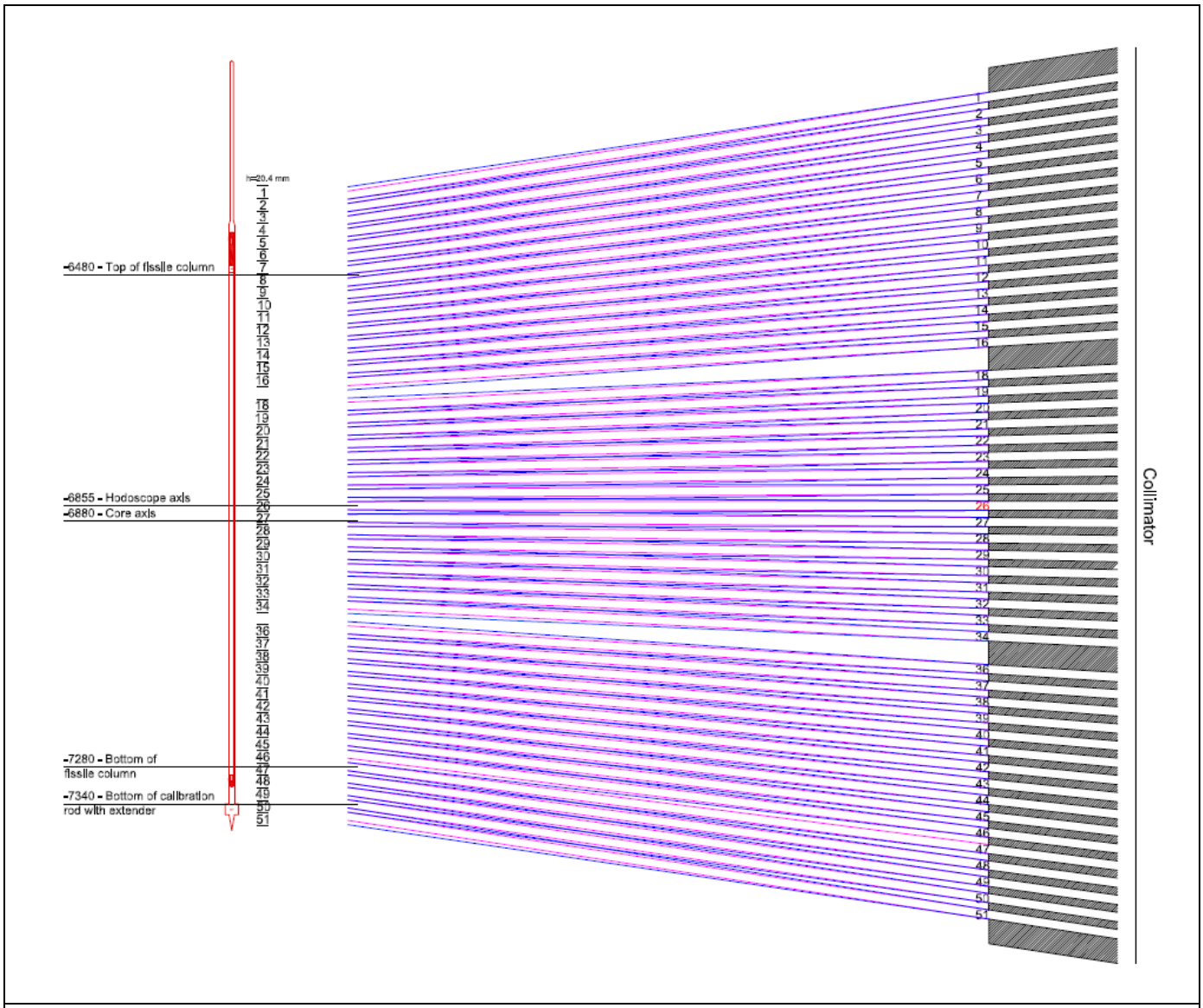

Figure 4:Rows of the hodoscope viewing CH1 rod

[2] Ground level of the reactor hall = 0 mm

However, the gamma activity is proportional to the flux of thermal neutrons from the core (Equation 4), that generates the radionuclides at the origin of gamma emissions. In addition, the flux of fast neutrons emitted by CH1 is proportional to the flux of thermal neutrons from the core. By transitivity, the gamma activity of the CH1 rod is proportional to the fast neutrons flux from CH1 that the PR and CF detectors measure. Consequently, the gamma activity corresponding, on the one hand to rows 1 to 8, and on the other hand, to rows 48 to 51, is in particular proportional to the fast neutrons fluxes emitted by the CH1 rod. This fast neutrons flux is obtained by a simulation with the MCNP code, developed by Los Alamos National Laboratory. An interpolation of the gamma measurements normalized with respect to the maximum is then carried out.
Furthermore, the normalized spectrometry values (^{103}Ru ray, 497 keV), and the normalized values obtained by MCNP for rows 1 to 8 and 48 to 51, are compiled, leading to an interpolated curve, g(z), called "spectro+MCNP" in Figure 5.

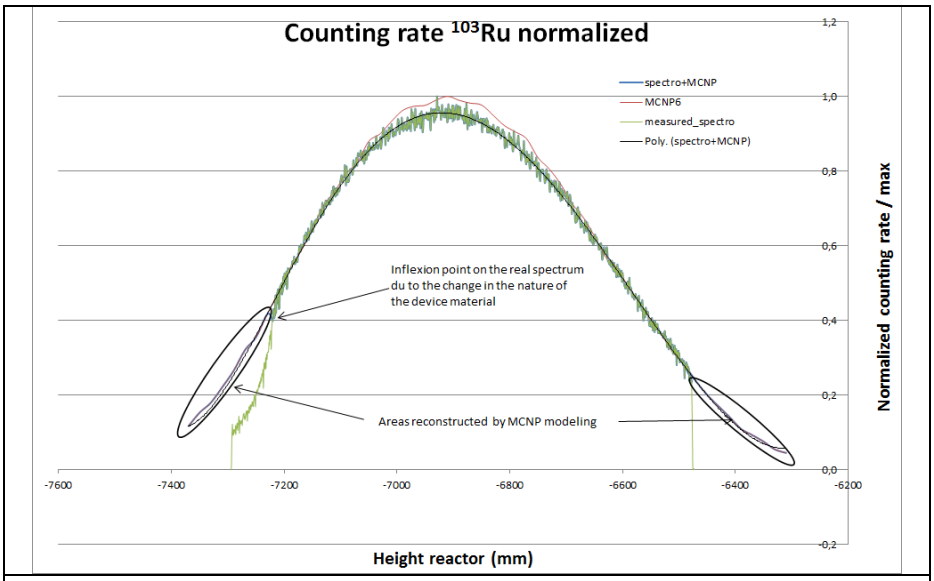

Figure 5 - Gamma spectrometry + MCNP calculation

VII. RELATION BETWEEN THE HODOSOCOPE DATA AND GAMMA SPECTROMETRY MEASUREMENTS

At this step, it is possible to determine the detector's sensitivity. Data measured by the hodoscope's detectors has been normalized in order to compare them to those obtained from gamma spectrometry. We

choose to normalize by average of the maximum counting rate, respectively for the PR and the FC. For each kind of detectors (PR and FC), normalization was performed using Equation 9 below.
Uncertainties linked to the counting rate were really low thanks to the high counting time.

$$T_{ij,n,}=\frac{T_{ij}}{<max(T_{ij})>} \text{ with } j = 1, 2, 3 \qquad \textbf{Equation 9}$$

Where:

- i = 1…51,
- j = 1, 2, 3, are respectively the left, center, right columns,
- $< max(T_{ij}) >$ is the average of the maximum counting rate,
- $T_{ij,n}$ is the normalized counting rate of the row i in a column j.

The normalized profile Ti,j,n (z) deduced from the hodoscope measurements, and the g(z) graph mentioned in VI are illustrated in the graph on Figure 6 for FC center, and Figure 7 for PR center below. We apply the same method for the others detectors (left PR, right PR, left FC, right FC)

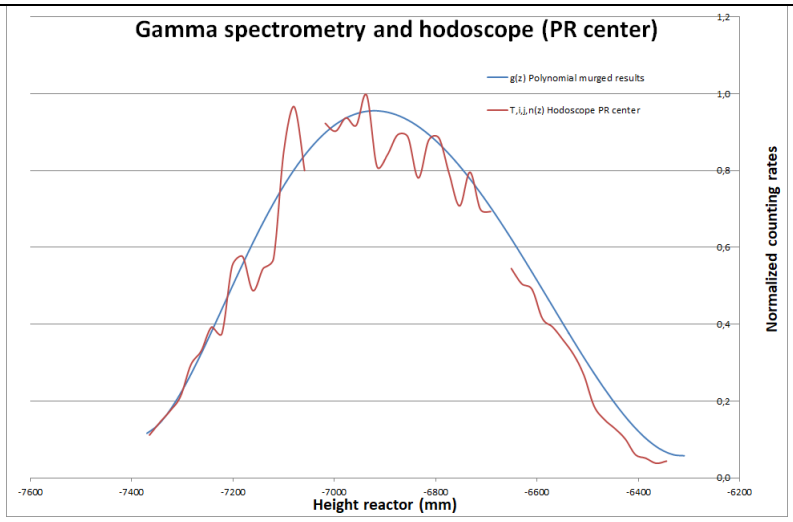

Figure 6: comparison between normalized profile deduced from the hodoscope measurements and gamma spectrometry profile merged with MCNP for FC

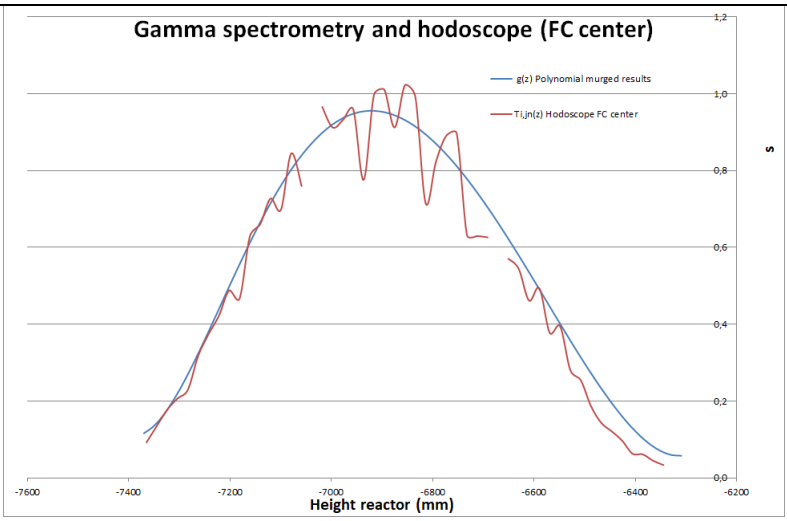

Figure 7: comparison between normalized profile deduced from the hodoscope measurements and gamma spectrometry profile merged with MCNP for PR

The sensitivity coefficients S(i,j) of the detectors are determined by a simple ratio between the normalized profile Ti,j,n (z) deduced from the hodoscope measurements, and the g(z) graph mentioned in VI, for corresponding detector located in z:

$$S_{i,j} = \frac{g(z)}{T_{i,j,n}(z)}$$

Where $S_{i,j}$ is the sensitivity coefficient of detector i in column j.

This procedure is implemented for the 3 columns (Left, Center, Right), whose profile is acquired by the hodoscope during the power plateau, and for the two types of detectors (PR and FC). It should be noticed that the counting rate is not measured by two detector rows, because the two corresponding line-of-sights (rows 17 and 35) are filled with stainless steel in order to strengthen the collimator.

VIII. RESULTS OF THE NEW CALIBRATION COEFFICIENTS

The difference between the old and new sensitivity coefficients is shown in Figure 8. Indeed, a calibration campaign was undertaken in 1994 with the sodium loop.
In this figure, it can be noticed that the difference is minimal on the lower part of the rod and maximum in the upper part. The maximum difference in the upper part is explained by the approximation induced by MCNP code, which is used to complete gamma spectrometry measurements [VI]. However, it should be noticed that lines 1 to 8 of the hodoscope are never used for a CABRI tests.

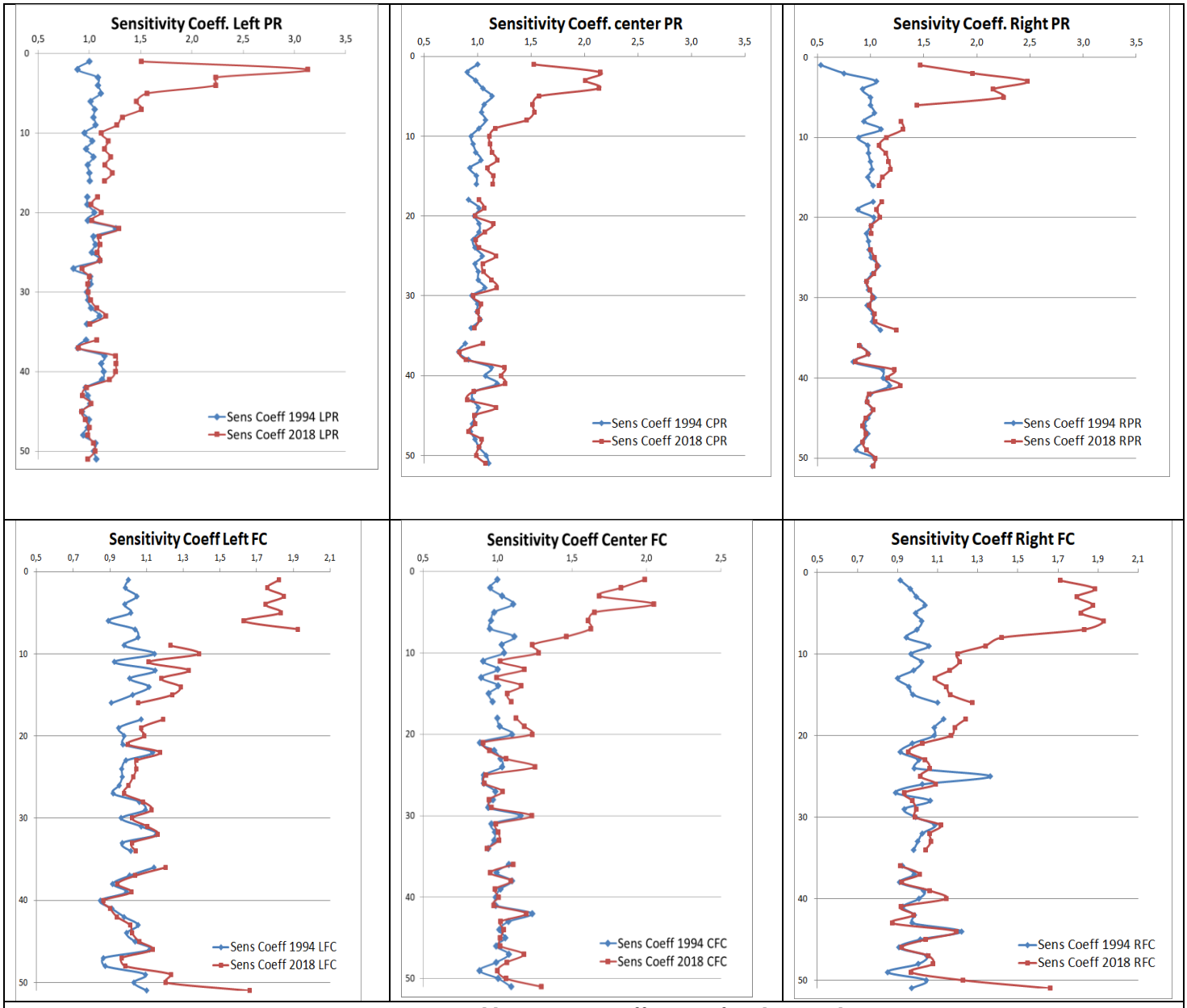

Figure 8 :New versus Old Sensitivity coefficients of Hodoscope detectors

IX. UNCERTAINTIES CALCULATION

The sensitivity coefficients are deduced from the ratio between the normalized gamma measurements (or the normalized MCNP calculation results for lines 1 to 8 and lines 48 to 51) and the normalized hodoscope counting rate. These measurements are independent, so the relative uncertainty is given by the following formula and are less than 3%:

$$\left(\frac{\sigma_S}{S}\right)^2 = \left(\frac{\sigma_{\tau\ Hod}}{\tau_{Hod}}\right)^2 + \left(\frac{\sigma_\Upsilon}{\Upsilon}\right)^2$$

Where:

$\left(\frac{\sigma_{\tau Hod}}{\tau_{Hod}}\right)^2$: is the relative uncertainty on the hodoscope detectors counting rate

And:

$\left(\frac{\sigma_\gamma}{\gamma}\right)^2$: is the relative uncertainty on the gamma measurements;

X. VALIDATION RESULTS

The hodoscope analysis software gives the possibility to compare the axial profiles using the old and new sensitivity coefficients applied on the same 10 MW power plateau (plateau performed for the hodoscope calibration). As shown in the Table 2 the new sensitivity coefficients lead to more regular axial profiles than those acquired with the old sensitivity coefficients (obtained in 1994 with the sodium loop).

Moreover, the new axial profiles are more consistent with the fast neutron flux. The new sensitivity coefficients lead to more consistent profiles also: as a matter of fact, for the collimator in "center" position, where the right and left columns must count the same number of fast neutrons, or in the "split" position where the CH1 rod is seen by center and left columns in the same manner, the new profiles overlap.

NB: In the graphs of Table 2, the measurements acquired are in green for the left column, in brown for the center one, and in pink for the right one.

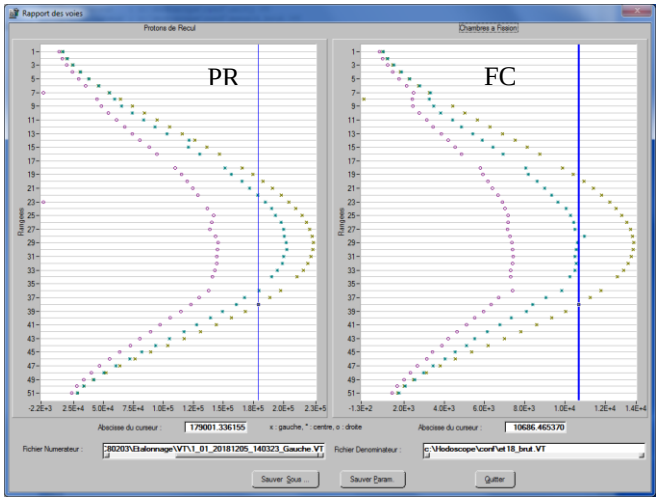	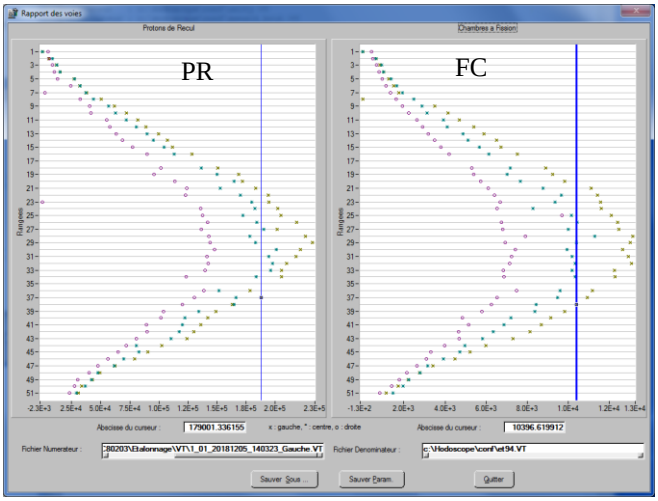
Axial profile obtained for PR and CF, using the **new** sensitivity coefficients with the collimator in left position	Axial profile obtained for PR and CF, using the old sensitivity coefficients with the collimator in left position
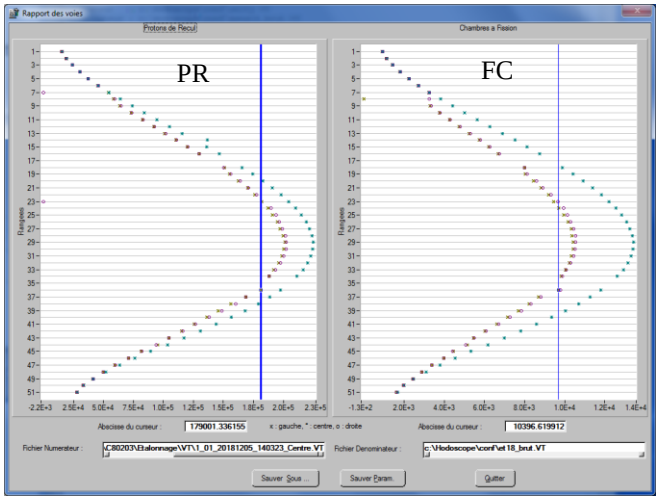	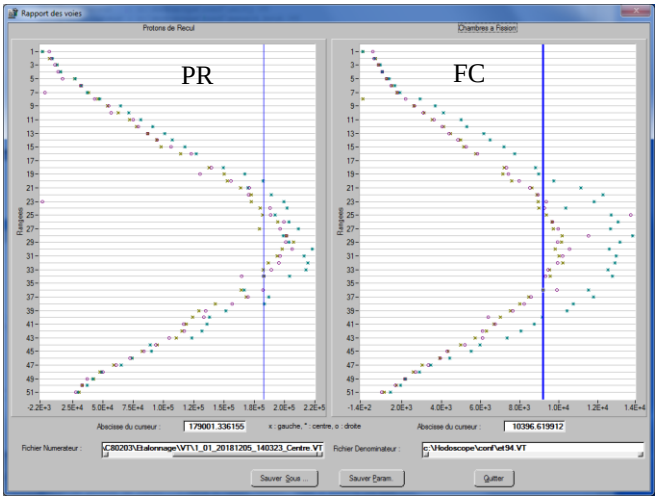
Axial profile obtained for PR and CF, using the new sensitivity coefficients with the collimator in center position	Axial profile obtained for PR and CF, using the old sensitivity coefficients with the collimator in center position

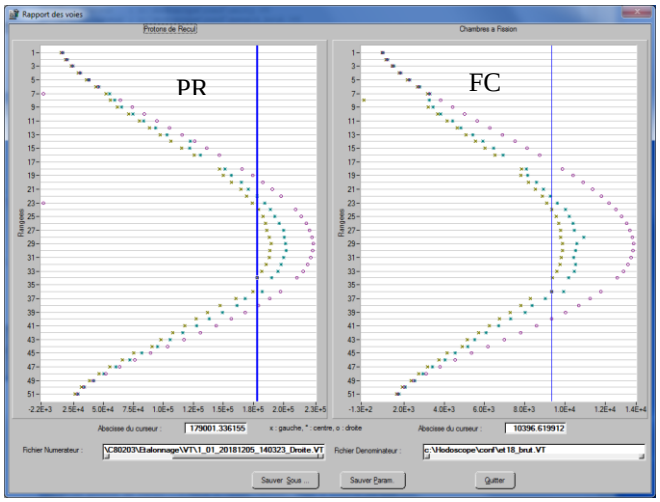	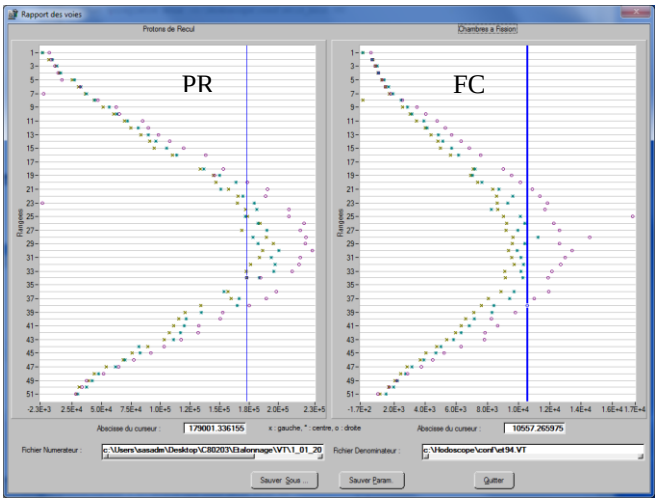
Axial profile obtained for PR and CF, using the new sensitivity coefficients with the collimator in right position	Axial profile obtained for PR and CF, using the old sensitivity coefficients with the collimator in right position
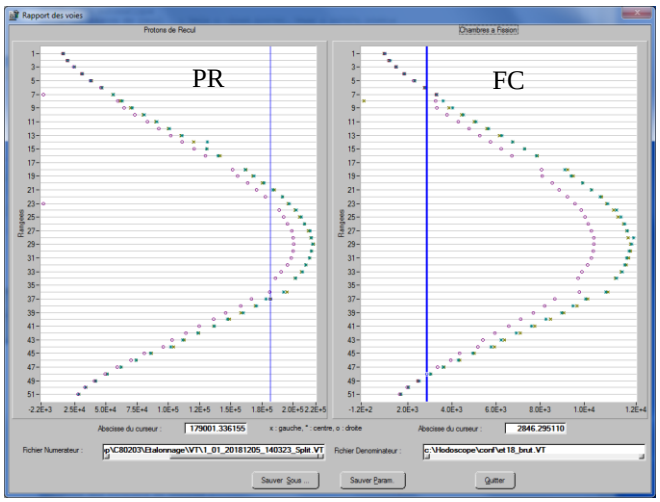	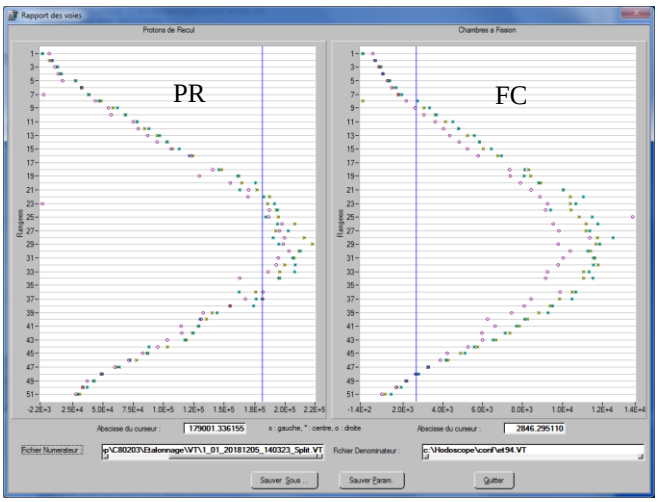
Axial profile obtained for PR and CF, using the new sensitivity coefficients with the collimator in split position	Axial profile obtained for PR and CF, using the old sensitivity coefficients with the collimator in split position

Table 2 :Axial profile for PR and CF on the four position of the collimator with the new sensitivity coefficients (left column) and the old one (right column)

XI. CONCLUSION

The calibration campaign of the hodoscope detectors performed in the period from October 2018 to march 2019 completed the all qualification phases of these specific experimental equipment implemented in the CABRI facility. Its aim was to obtain the new sensitivity coefficients of the detectors. The originality of the method was to use firstly fast prompt neutrons produced by fission produced into a fresh UO2 fuel rod (calibration rod) in CABRI reactor, detected by the hodoscope, and in second time, to measure in hot cells facility, one delayed gamma ray emitted by fission products, which were produced by fission in the calibration rod.

The new sensibility coefficients of the detectors will be used now for the analysis of all experimental program performed in the CABRI facility.

XII. REFERENCES

[1]. B. Duc, B. Biard, P. Debias, L. Pantera, J.-P. Hudelot and F. Rodiac, "Renovation, improvement and experimental validation of the Helium-3 transient rods system for the reactivity injection in the CABRI reactor," IGORR 2014 Conference, Bariloche, Argentina, November 2014.

[2]. S.Mirotta, J.Guillot, V.Chevalier and B.Biard, "Qualification and characterization of electronics of the fast neutrons Hodoscope detectors using neutrons from CABRI core," In ANIMMA2017 Conference Proceedings, Liege, June 2017.

[3]. Bruno Biard, Vincent Chevalier, Claude Gaillard, Vincent Georgenthum, Quentin Grando, Jérôme Guillot, Lena Lebreton, Christelle Manenc, Salvatore Mirotta, Nathalie Monchalin “Reactivity Initiated Accident transient testing on irradiated fuel rods in PWR conditions: The CABRI International Program » Annals of Nuclear